Wave Motion 136 (2025) 103530

Contents lists available at ScienceDirect

Wave Motion

journal homepage: www.elsevier.com/locate/wamot

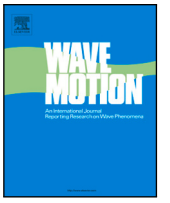

Floquet scattering of shallow water waves by a vertically oscillating plate

Magdalini Koukouraki [a,*], Philippe Petitjeans [a], Agnès Maurel [b], Vincent Pagneux [c]

[a] Laboratoire de Physique et Mécanique des Milieux Hétérogènes, ESPCI-Paris, Sorbonne Université, Université Paris Cité, CNRS, Paris, 75005, France
[b] Institut Langevin, ESPCI-Paris, CNRS, Paris, 75005, France
[c] Laboratoire d'Acoustique de l'Université du Mans, Le Mans Université, CNRS, Le Mans, 72085, France

ARTICLE INFO

Keywords:
Water waves
Floquet scattering
Time-varying topography
Oscillating plate

ABSTRACT

We report on the scattering of a plane wave from a vertically oscillating plate in the low frequency approximation by means of Floquet theory. In the case of a static plate, the scattering coefficients are evaluated via mode matching method for the full two-dimensional linearized water wave problem and are compared with the coefficients obtained from a reduced one-dimensional model in the shallow water approximation. The main part of the analysis is the extension of this 1D shallow water approximation to the case of a vertically oscillating plate, where time modulation is only encapsulated in the blockage coefficient. We show that the incident wave is scattered into Floquet sidebands and extract the scattering coefficients for each harmonic using a Floquet scattering formalism. Finally, considering a slowly oscillating plate, we propose a quasistatic approximation which appears to be particularly accurate.

1. Introduction

Time-dependent systems involving wave-matter interactions have been extensively studied over the years, as they encompass intriguing wave phenomena which are universal from quantum mechanics to condensed matter and fluid mechanics [1–4]. These effects include time reversal [5], frequency conversion [6], parametric amplification [7], transient amplification [8], temporal waveguiding [9] among many others. An increasing activity regarding time-varying media concerns electromagnetic platforms; it dates back to the pioneering works of Morgenthaler in the 1950s [10] on waves passing through media where the phase velocity is rapidly modified. Thenceforth, the research on time-varying metamaterials as a means to control and harness waves has significantly grown [11]. Understanding the interaction of waves with scatterers exhibiting time-variation can be challenging and often requires the development of new theoretical and numerical tools. Floquet theory [12] has been long applied for scattering problems in periodically driven systems, denoted as Floquet scattering as discussed in [13,14] for the transmission of electrons through harmonically modulated potentials and in [15] for the propagation of waves in layered optomagnonic structures.

In the realm of water waves, the bathymetry can play a key role in the wave dynamics and thus has been a topic of interest for many years in terms of wave scattering. More specifically, the reflection and transmission of waves by different bottom profiles has been already examined through the conformal mapping technique, which was first proposed by Fitz-Gerald (1976) [16] and Hamilton (1977) [17], and afterwards implemented by Evans and Linton (1994) [18]. This technique relies on using a conformal transformation which enables to map an initial fluid domain with an irregular bottom boundary into a constant strip of fluid with the

* Corresponding author.
E-mail address: magdalini.koukouraki@espci.fr (M. Koukouraki).

https://doi.org/10.1016/j.wavemoti.2025.103530
Received 26 November 2024; Accepted 19 February 2025
Available online 1 March 2025

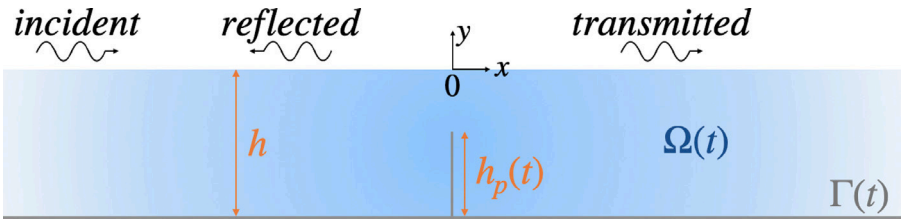

Fig. 1. Schematic representation of wave scattering by an infinitely thin plate of height $h_p(t)$ inside a channel of depth h.

only added implication being an extra coefficient at the surface condition. Porter (2005) [19] subsequently revisited the technique to account for steep components in the bottom profile, concentrating on Roseau, shoaling and ridge-type profiles.

For the particular bathymetry with vertical barriers, numerous theoretical works have been made on wave scattering in infinitely-deep water [20,21] and on structured beds composed of periodically arranged vertical plates in shallow water [22–24]. Even though the forementioned literature involves static plates, there have also been works on moving underwater barriers and time-varying topographies. Evans (1970) in [25] reports on the forces and moments on a vertical plate performing rolling oscillations under the water surface. Also, Tuck (1977) in [26] treats the general scattering problem of water waves from a space–time dependent bottom profile in the shallow water approximation where the wavelength is much larger than the water depth, by using matched asymptotic expansions.

In this study, we focus on the linear long-wavelength water wave theory and we wish to model the interaction of a monochromatic wave with a submerged infinitely thin vertical plate, whose height is a function of time. First, we formulate the problem where the plate is static and then we proceed to the case where the plate is vertically oscillating. For the static plate, we present the full linearized problem and extract the two-dimensional field and the scattering coefficients for all range of frequencies. Then, by moving from the mid to the low frequency range of shallow water approximation, the field can be described effectively by the one-dimensional wave equation where the effect of the plate is incorporated in jump conditions at the plate position. For the vertically oscillating plate and in this low-frequency limit, we propose a Floquet theory approach in order to retrieve the reflected and transmitted fields, as well as a quasistatic approximation for the case where the plate is oscillating sufficiently slow compared to the period of the incident wave. Finally, we discuss the two methods in terms of their agreement and limitations.

2. Scattering by a submerged vertical plate

2.1. Governing equations

Let us consider the irrotational flow of an incompressible and inviscid fluid of depth h, extending horizontally in an unbounded domain, and an infinitely thin plate of height h_p sitting at the fluid bottom at position $x = 0$, as depicted in Fig. 1. We wish to characterize the scattering problem of a plane wave, incident on the plate from $x = -\infty$, when the plate height can also be allowed to vary with time. Following the classical linearized water-wave theory, which is addressed in one of the textbooks [27–30], the problem translates as:

$$\begin{cases} \Delta\Phi = 0, \quad \text{in} \quad \Omega(t) \\ \hat{\mathrm{n}} \cdot \nabla\Phi = 0, \quad \text{on} \quad \Gamma(t) \\ \frac{\partial\Phi}{\partial y} = -\frac{1}{g}\frac{\partial^2\Phi}{\partial t^2}, \quad y = 0, \end{cases} \tag{1}$$

where $\Phi(x, y, t)$ denotes the velocity potential, g the acceleration of gravity and $\hat{\mathrm{n}}$ the unit normal vector on $\Gamma(t)$. Note that by assuming that the plate has an infinitely small width, we guarantee that the plate will not act as a source when vertically oscillating (see Mei [27]). This is evident from the absence of a source term on the impermeable boundary condition on $\Gamma(t)$.

2.2. Shallow water model with jump conditions

As demonstrated in [26], by starting from the system (1) and implementing matched asymptotic expansions, one can eliminate the wave-field dependence on y in the long-wavelength limit and obtain a reduced one-dimensional model with jump conditions at the position of the plate. This model reads as

$$\frac{\partial^2\phi}{\partial x^2} - \frac{1}{c_0^2}\frac{\partial^2\phi}{\partial t^2} = 0, \tag{2a}$$

$$[\phi]_{0^-}^{0^+} = 2B_\mu(t)h\partial_x\phi\Big|_0, \quad \left[\partial_x\phi\right]_{0^-}^{0^+} = 0, \tag{2b}$$

where $\phi(x, t) = \Phi(x, 0, t)$ is now the y-independent velocity potential, $c_0 = \sqrt{gh}$ is the velocity at which long waves propagate and B_μ is known as the blockage coefficient. B_μ is determined strictly from the geometrical profile of the fluid bottom and is a function

of time when the topography is time-varying. For an infinitely thin plate, the blockage coefficient is given in the following explicit form:

$$B_\mu(t) = -\frac{2}{\pi}\ln\left[\sin\left(\frac{\pi}{2}(1-\mu(t))\right)\right], \quad \mu = \frac{h_p(t)}{h}, \tag{3}$$

where $h_p(t)$ is the height of the oscillating vertical plate. Further information on the derivation of Eq. (3) can be found in the paper [19].

3. The static plate

First, as a warm-up and in order to assess the validity range of the shallow water approximation, we are going to tackle the scattering problem for a static plate.

3.1. Mode matching method for any water depth regime

In order to determine the reflection R and transmission T coefficients in the time-harmonic regime (convention $e^{-i\omega t}$) for each dimensionless frequency $\omega\sqrt{h/g}$ of the incident wave we follow the mode matching method. Although this method is already discussed in [27], in this section we revisit its key points for our case, where the scatterer is an infinitely thin vertical plate.

First, we rewrite the system (1) in its time-independent form, by setting $\Phi = \Re\{\tilde{\Phi}e^{-i\omega t}\}$ and then dropping the tilde:

$$\begin{cases} \Delta\Phi = 0, \quad \text{in} \quad \Omega \\ \hat{\mathrm{n}}\cdot\nabla\Phi = 0, \quad \text{on} \quad \Gamma \\ \frac{\partial\Phi}{\partial y} = \frac{\omega^2}{g}\Phi, \quad y = 0. \end{cases} \tag{4}$$

We start by expanding the solution (for $x \neq 0$) on the basis of orthonormal transverse eigenfunctions $g_n(y)$, $n \geq 0$, which by solving the system (4) are found to be

$$g_n(y) = G_n\cosh[k_n(y+h)], \quad G_n = \sqrt{\frac{\sinh(2k_nh)}{4k_n} + \frac{h}{2}}, \tag{5}$$

with k_n the roots of the dispersion relation

$$\omega^2 = gk\tanh kh, \tag{6}$$

with k_0 the positive real solution and k_n the purely imaginary ones for $n \geq 1$ with positive imaginary parts. The above functions satisfy both the Robin-type condition at $y = 0$, and the Neumann boundary condition at $y = -h$. Therefore, the most general solution of the scattering problem reads as

$$\Phi(x<0,y) = (e^{ik_0x} + Re^{-ik_0x})g_0(y) + \sum_{n=1}^{\infty} A_n e^{-ik_nx}g_n(y), \tag{7}$$

$$\Phi(x>0,y) = Te^{ik_0x}g_0(y) + \sum_{n=1}^{\infty} B_n e^{ik_nx}g_n(y), \tag{8}$$

with R and T the reflection and transmission coefficients of the plane wave mode respectively and A_n and B_n are the coefficients of the evanescent modes which are excited near the plate. By looking at the symmetry of the problem, it is straightforward to split it into two sub-problems: a symmetric and an antisymmetric part,

$$\Phi = \Phi_s + \Phi_a, \quad \text{with} \quad \Phi_s(x,y) = \Phi_s(-x,y), \quad \Phi_a(x,y) = -\Phi_a(-x,y), \tag{9}$$

where we use the subscript "s" for symmetric and "a" for antisymmetric. We then need to solve the problem just at the region $x < 0$ and extend the solution for $x > 0$.

Due to symmetries, on the one hand, the boundary conditions which should be satisfied at $x = 0$ are respectively

$$\frac{\partial\Phi_s}{\partial x}(x=0,S^-) = \Phi_a(x=0,S^-) = 0, \tag{10}$$

for the surface $S^- = \{x = 0, y \in [-(h-h_p),0]\}$ above the plate.

On the other hand, the impermeability condition along the rigid surface of the plate $S_p = \{x = 0, y \in [-h,-(h-h_p)]\}$ yields

$$\frac{\partial\Phi_s}{\partial x}(x=0,S_p) = \frac{\partial\Phi_a}{\partial x}(x=0,S_p) = 0. \tag{11}$$

Therefore, we use the following expansion for the left region with respect to the plate:

$$\Phi_{s,a}(x<0,y) = (e^{ik_0x} + R_{s,a}e^{-ik_0x})g_0(y) + \sum_{n=1}^{\infty} A_n e^{-ik_nx}g_n(y), \tag{12}$$

where $R_{s,a}$ denote the reflection coefficients of each subproblem and it can be shown that

$$R = \frac{1}{2}\left(R_s + R_a\right), \quad T = \frac{1}{2}\left(R_s - R_a\right), \tag{13}$$

with $|R_{s,a}| = 1$ because of energy conservation. The symmetric part has a trivial solution, since the Neumann boundary condition at $S = S_p \bigcup S^-$ yield $R_s = 1$. Hence, the only part which contributes to the variation of the scattering coefficients with frequency is R_a, the antisymmetric one.

It is convenient to write the antisymmetric part of solution (12) in a more general form, such as

$$\Phi_a(x \le 0, y) = \sum_{n=0}^{\infty} a_n(x) g_n(y), \tag{14}$$

where we decompose the coefficients a_n into the ones of the incoming wave and of the reflected wave,

$$a_n(x) = a_{n,0}(x) + a_{n,r}(x), \tag{15}$$

with $a_{n,0}(x) = \delta_{0n} e^{ik_0 x}$ and $a_{n,r}(x) = C_n e^{-ik_n x}$. Next, we apply condition (10) for the component $\Phi_a(x = 0, S^-)$, and project over the transverse functions

$$\hat{g}_p(y) = \hat{G}_p \cosh[\hat{k}_p(y + (h - h_p))], \quad \hat{G}_p = \sqrt{\frac{\sinh(2\hat{k}_p(h - h_p))}{4\hat{k}_p} + \frac{(h - h_p)}{2}}, \tag{16}$$

with $\hat{k}_p$ satisfying $\omega^2 = g\hat{k}\tanh\hat{k}(h - h_p)$. Doing so we obtain

$$\mathrm{F}^{\mathrm{t}}\mathbf{a}(0) = 0, \tag{17}$$

with the vector $\mathbf{a}(0)$ containing the components $a_n(x = 0)$ and the matrix elements of F are given as

$$(\mathrm{F})_{mp} = \int_{-(h-h_p)}^{0} g_m(y)\hat{g}_p(y)dy. \tag{18}$$

Then, we can rewrite the continuity condition of $\partial_x \Phi_a$ at $x = 0$ as

$$\partial_x \Phi_a|_{x=0} = \begin{cases} 0, & \text{at} \quad S_p \\ \sum_{p=0}^{\infty} c_p \hat{g}_p(y), & \text{at} \quad S^-. \end{cases} \tag{19}$$

Deriving Eq. (14) with respect to x, using Eq. (19), and projecting on the functions g_m we have that

$$\mathbf{a}'(0) = \mathrm{F}\mathbf{c}. \tag{20}$$

Taking the derivative of a_n in Eq. (15), we have

$$\mathbf{a}'(0) = \mathrm{Y}(\mathbf{a_0}(0) - \mathbf{a_r}(0)), \tag{21}$$

where $(\mathbf{a_0})_m = \delta_{m0}$ and Y a diagonal matrix with elements $(\mathrm{Y})_{m,m'} = ik_m\delta_{m,m'}$. Next, a simple manipulation of Eqs. (15) and (17) yields the relation

$$\mathrm{F}^{\mathrm{t}}\mathbf{a_r}(0) = -\mathrm{F}^{\mathrm{t}}\mathbf{a_0}(0). \tag{22}$$

Finally, combining Eqs. (22), (20) and (21) one can extract that

$$\mathbf{a_r}(0) = \mathbf{a_0}(0) - \mathrm{Y}^{-1}\mathrm{F}\mathbf{c}, \tag{23}$$

where

$$\mathbf{c} = 2(\mathrm{F}^{\mathrm{t}}\mathrm{YF})^{-1}\mathrm{F}^{\mathrm{t}}\mathbf{a_0}(0). \tag{24}$$

Computing Eqs. (23) and (24) numerically and using a number of modes around $N = 50$ for the expansion on $S(N, g_n)$ and a number $P \sim (S^-/S)N$ for the expansion on $S^-(P, \hat{g}_p)$, we retrieve R and T as well as the full wave field for each frequency. In Fig. 2 we show the two-dimensional field recovered for ratio $\mu = 0.5$ and two water depth regimes: the finite-water depth and the shallow water limit. As illustrated, the wave field becomes almost homogeneous with y when $\omega\sqrt{h/g} \ll 1$ (notice the variation of the colorbar on panel (b)), which justifies simplifying the set of Eqs. (4) to just one partial differential equation at the surface supplemented with the effective boundary conditions at $x = 0$.

3.2. Low frequency approximation: the shallow water regime

As was previously discussed, for waves of sufficiently small amplitude (linear regime) and of very long wavelength compared to the water depth (shallow water regime), the wave dynamics can be well approximated by the wave equation (2a). In this shallow water approximation (SWA), waves are nondispersive and satisfy the dispersion relation $\omega = c_0 k$, with k the wave number.

Considering once again the harmonic regime, so that $\phi = \Re\{f(x)e^{-i\omega t}\}$, and a non-moving plate, such that $B_\mu(t) = \text{const}$ in Eq. (2b), we construct the solution of Eq. (2a) as follows: For $x < 0$, the wave is composed of an incident, right-propagating, wave and a reflected wave, $f^- = e^{ikx} + R_{sw}e^{-ikx}$, while for $x > 0$ the solution takes the form of a transmitted wave, $f^+ = T_{sw}e^{ikx}$. By using

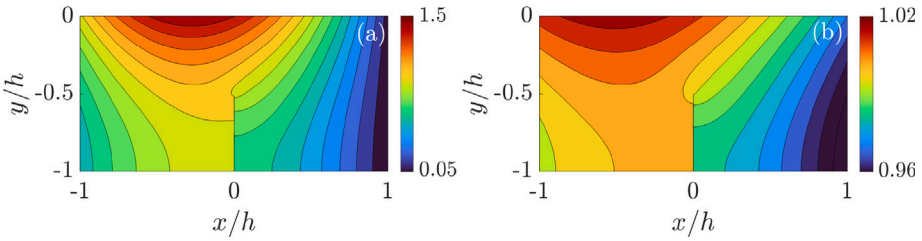

Fig. 2. Two-dimensional profile of the wave field recovered via mode-matching method for **(a)** $\mu = 0.5$, $\omega\sqrt{h/g} = 1$ and **(b)** $\mu = 0.5$, $\omega\sqrt{h/g} = 0.2$.

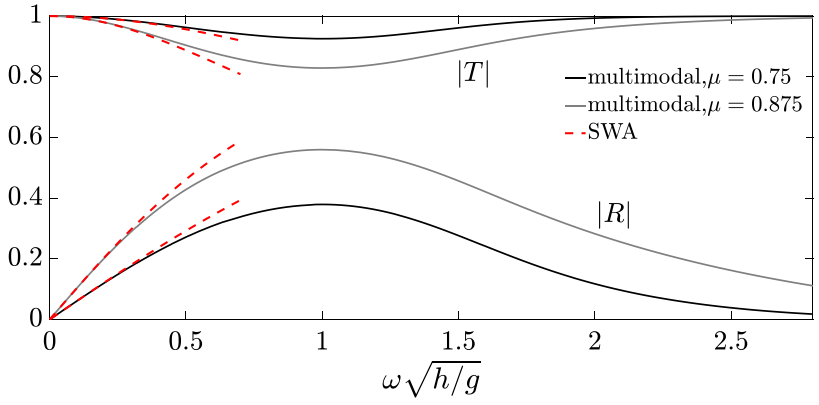

Fig. 3. Variation of $|R|$ and $|T|$ for $\mu = 0.75$ and $\mu = 0.875$. The shallow water approximation (SWA) is given by Eq. (25).

these expressions for f^+ and f^- when applying the continuity of $\partial_x\phi$ and the jump condition of ϕ at $x = 0$ (Eq. (2b)), we obtain the reflection and transmission coefficient in the shallow water approximation as

$$R_{sw} = -\frac{ikhB_\mu}{1 - ikhB_\mu}, \quad T_{sw} = \frac{1}{1 - ikhB_\mu}. \tag{25}$$

Notice that these scattering coefficients satisfy the energy conservation $|R_{sw}|^2 + |T_{sw}|^2 = 1$.

In Fig. 3, we portray R and T obtained from the mode matching method along with the relations (25) with respect to the frequency for two values of μ. Notice that the reflection increases as the plate height approaches the surface (increasing μ). Furthermore, the SWA holds sufficiently up to $\omega\sqrt{h/g} = 0.2$, which leads us to establish a frequency interval of $\omega\sqrt{h/g} \in [0, 0.5]$ for our study in the shallow water limit.

4. The vertically oscillating plate: shallow water regime

Now, we are going to the main part of this work where we evaluate the scattering by a vertically oscillating plate in the shallow water approximation.

4.1. Floquet theory

In this paper we are interested in the simplest case where the time variation is introduced in the blockage coefficient. We hereafter consider that

$$B_\mu(t) = B_{\mu,0} + B_{\mu,1}\cos(\omega_p t), \tag{26}$$

with ω_p the characteristic parameter of oscillation, which consequently leads to a more complex plate motion, defined as

$$\mu(t) = 1 - \frac{2}{\pi}\arcsin\left[\exp\left(-\frac{\pi}{2}B_\mu(t)\right)\right]. \tag{27}$$

Our starting point is the problem already introduced in Section 2.2 with a right-propagating monochromatic wave of frequency ω impinging on the periodically driven scatterer. First, Floquet theorem [12,31] allows us to write the solution in the form

$$\phi = \Re\{e^{-i\omega t}\psi\}, \quad \psi(x,t) = \psi(x, t + T_p), \tag{28}$$

with $T_p = 2\pi/\omega_p$. Since ψ is periodic, it can be expanded in the Fourier series

$$\psi(x,t) = \sum_n \psi_n(x) e^{-in\omega_p t}, \tag{29}$$

with $n \in (-\infty, +\infty)$ and the Fourier modes $e^{-in\omega_p t}$ satisfying the orthogonality relation:

$$\frac{1}{T_p}\int_0^{T_p} e^{i(m-n)\omega_p t} dt = \delta_{mn}. \tag{30}$$

Substituting Eqs. (28) and (29) into Eq. (2a), projecting on $e^{-in\omega_p t}$ and using Eq. (30), we find for $x \neq 0$ that

$$\frac{d^2\psi_n}{dx^2} + k_n^2 \psi_n = 0, \quad k_n = \frac{\omega_n}{c_0}, \tag{31}$$

where $\omega_n = \omega + n\omega_p$. It follows from Eq. (2b) that the boundary condition for ψ_n reads as:

$$[\psi_n']_{0^-}^{0^+} = 0, \quad [\psi_n]_{0^-}^{0^+} = 2B_{\mu,0} h \psi_n' + B_{\mu,1} h(\psi_{n+1}' + \psi_{n-1}'). \tag{32}$$

Hence, one can write the solution for ψ_n in the regions $x < 0$ and $x > 0$ as follows:

$$\psi_n^-(x<0) = \delta_{0n} e^{ik_n x} + r_n e^{-ik_n x}, \tag{33}$$

$$\psi_n^+(x>0) = t_n e^{ik_n x}, \tag{34}$$

with r_n and t_n the scattering coefficients of each harmonic. The next step is to evaluate the jump conditions by substituting Eqs. (33) and (34) in Eq. (2b), in order to derive the expressions for r_n and t_n. First, we proceed with the continuity of $\partial_x \phi$ at $x = 0$, which yields

$$\sum_n (\delta_{0n} - r_n) k_n e^{-in\omega_p t} = \sum_n t_n k_n e^{-in\omega_p t}. \tag{35}$$

By projecting on the Fourier modes, using the orthogonality relation (30), and representing the scattering coefficients in vector forms, with vector components $(\mathbf{t})_m = t_m$, $(\mathbf{r})_m = r_m$, we find that

$$\mathbf{t} = \mathbf{b} - \mathbf{r}, \tag{36}$$

where $(\mathbf{b})_m = \delta_{0m}$. Notice that $r_m = -t_m$, for $m \neq 0$, which is consistent with the symmetry of the problem.

Then, the discontinuity of ϕ at $x = 0$ translates into

$$\begin{aligned} &\sum_n \left(t_n - \delta_{0n} - r_n\right) e^{-in\omega_p t} = \\ &\sum_n ik_n \left(\delta_{0n} - r_n\right) \left[2B_{\mu,0} h e^{-in\omega_p t} + B_{\mu,1} h \left(e^{-i(n-1)\omega_p t} + e^{-i(n+1)\omega_p t}\right)\right], \end{aligned} \tag{37}$$

which after following the same procedure as before can be adapted into a form of a linear system:

$$\mathbf{t} = (\mathrm{I} + \mathrm{V})\mathbf{b} + (\mathrm{I} - \mathrm{V})\mathbf{r}, \tag{38}$$

with

$$(\mathrm{V})_{m,m'} = iB_{\mu,1} h \left(k_{m'+1}\delta_{m,m'+1} + k_{m'-1}\delta_{m,m'-1}\right) + 2iB_{\mu,0} h k_{m'} \delta_{m,m'}, \tag{39}$$

and I denoting the identity matrix. Since V induces coupling between the harmonics, Eq. (38) demonstrates the fact that the incident wave is scattered into Floquet sidebands with frequencies ω_n. Substituting Eq. (36) into Eq. (38) we obtain the relation

$$\mathbf{r} = -(2\mathrm{I} - \mathrm{V})^{-1}\mathrm{V}\mathbf{b}. \tag{40}$$

Finally, by performing some algebraic manipulations combining the boundary conditions (32) for ψ_n and the form of solutions for ψ_n given in Eqs. (33) and (34), one can derive the conservation of the quantity

$$\mathcal{T} + \mathcal{R} = 1, \tag{41}$$

with $\mathcal{T} = \sum_n |t_n|^2 k_n/k_0$, and $\mathcal{R} = \sum_n |r_n|^2 k_n/k_0$. More precisely, for this derivation one needs to proceed as follows. First, one evaluates the discontinuity of the product $\bar{\psi}_n \psi_n'$ at $x = 0$ using Eq. (32):

$$[\bar{\psi}_n \psi_n']_{0^-}^{0^+} = \left[2B_{\mu,0} h \bar{\psi}_n'(0) + B_{\mu,1} h \left(\bar{\psi}_{n+1}'(0) + \bar{\psi}_{n-1}'(0)\right)\right] \psi_n'(0). \tag{42}$$

Then, one takes the sum of this product over all n-harmonics which gives

$$[\sum_n \bar{\psi}_n \psi_n']_{0^-}^{0^+} = 2B_{\mu,0} h \sum_n |\psi_n'(0)|^2 + B_{\mu,1} h \sum_n \left(\psi_n'(0)\bar{\psi}_{n+1}'(0) + \bar{\psi}_{n-1}'(0)\psi_n'(0)\right). \tag{43}$$

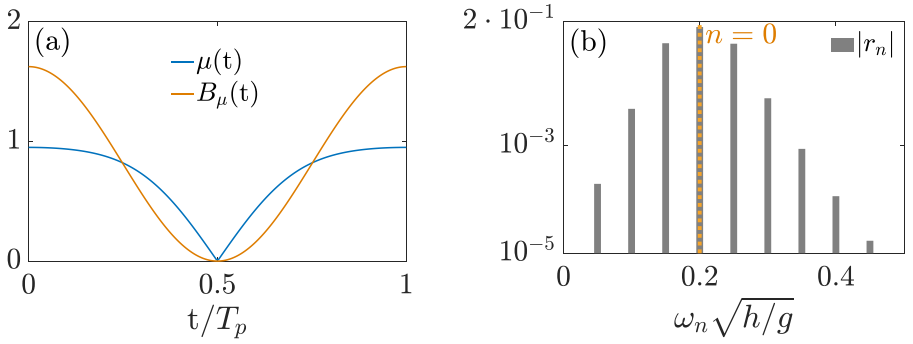

Fig. 4. (**a**) Temporal variation of the blockage coefficient in one period T_p, and the corresponding plate oscillation. (**b**) Reflection coefficients of the generated harmonics for the plate oscillation of panel (a), with $\omega\sqrt{h/g} = 0.2$ and $\omega_p = \omega/4$.

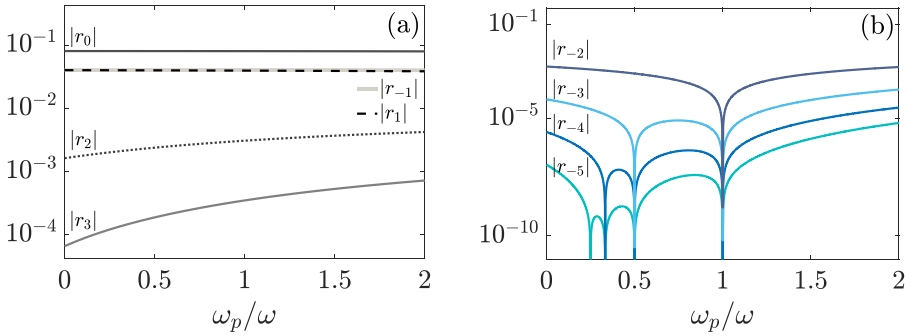

Fig. 5. Variation of the reflection coefficient of each harmonic in terms of ω_p normalized by the fixed incident frequency $\omega\sqrt{h/g} = 0.1$, for $-1 \le n \le 3$ in (**a**), and for $-5 \le n \le -2$ in (**b**).

Rewriting that $\sum_n \bar{\psi}'_{n-1}\psi'_n = \sum_n \bar{\psi}'_n\psi'_{n+1} + \bar{\psi}'_{-N-1}\psi'_{-N} - \bar{\psi}'_N\psi'_{N+1}$ and given than $\psi_{-N-1} = \psi_{N+1} = 0$, since $n \in [-N, N]$, Eq. (43) takes the form

$$[\sum_n \bar{\psi}_n\psi'_n]_{0^-}^{0+} = 2B_{\mu,0}h\sum_n |\psi'_n(0)|^2 + 2B_{\mu,1}h\sum_n \Re\{\psi'_n(0)\bar{\psi}'_{n+1}(0)\}. \tag{44}$$

From there one finds that

$$[\Im\{\sum_n \bar{\psi}_n\psi'_n\}]_{0^-}^{0+} = 0, \tag{45}$$

which indicates the conservation of the total flux at $x = 0$. Furthermore, since the total flux is also conserved for $x < 0$ and $x > 0$ separately, a property stemming from Eq. (31), it is conserved everywhere in space: $[\Im\{\sum_n \bar{\psi}_n\psi'_n\}]_{-\infty}^{+\infty} = 0$. In the end one obtains Eq. (41). Incidentally, this conservation law is also found in the case of the Schrödinger equation (see [15]), referring to the probability current conservation, with $\mathcal{T}$ the transmittance and $\mathcal{R}$ the reflectance.

4.1.1. Generation of harmonics

Equipped with Eqs. (36) and (40), we can now investigate and quantify the harmonic generation. In order for the plate to have a visible impact on the wave at low frequencies, we choose to impose a strong vertical plate movement as shown in Fig. 4a, where $\mu(t) \in [0, 0.95]$. For this configuration, and setting $\omega\sqrt{h/g} = 0.2$ and $\omega_p = \omega/4$, the harmonics which are produced at $n = \pm 1$ represent roughly 49% of the fundamental one in terms of reflection, while at each higher order of n the coefficient $|r_n|$ drops an order of magnitude (see Fig. 4b). While in this example we witness an important contribution of the first sidebands ($n = \pm 1$) in the total reflected field, we wish to see if this is still true for different frequencies of oscillation. For this purpose we fix the frequency of the incident wave and vary ω_p, so as to uncover how each harmonic is affected by this variation.

In Fig. 5 we depict a numerical application, where $\omega\sqrt{h/g} = 0.1$ and $\omega_p\sqrt{h/g} \in [0, 0.5]$, plotting the harmonics corresponding to $-1 \le n \le 3$ on panel (a) and $-5 \le n \le -2$ on panel (b). It is clear that the harmonics with $n \ge -1$ are monotonic with ω_p/ω, and that the dependence on the plate oscillation decreases as we move from $n = 3$ towards the fundamental harmonic, which appears constant compared to its counterparts. The first sidebands at $n = \pm 1$ are almost identical, and we find that $|r_{-1}| \simeq |r_1|$ as $\omega_p/\omega \to 0$, which will be explained in the following section concentrating on the quasistatic adiabatic limit. Interestingly, on panel (b) we observe the elimination of all r_n with $n < -1$ at $\omega = \omega_p$ and the elimination of all r_n with $n < -2$ at $\omega = 2\omega_p$.

In fact, it appears that

$$|r_n| = 0, \quad \text{for} \quad n < -m, \quad \text{when} \quad \omega = m\omega_p, \tag{46}$$

with $m \in \mathrm{N}^*$, $n \in \mathrm{Z}$. Indeed, at these frequencies the system (40) decouples and explicit relations can be found for $n \geq -m$. For instance, for $m = 1$ one can extract that

$$r_{-1} = \frac{iB_{\mu,1}hk_0}{2}(r_0 - 1), \tag{47}$$

$$r_1 = \frac{iB_{\mu,0}hk_0 + r_0\left(1 - iB_{\mu,0}hk_0\right)}{iB_{\mu,1}hk_0}, \tag{48}$$

$$r_2 = -\frac{\left\{2iB_{\mu,0}hk_0 + (4B_{\mu,0}^2 - B_{\mu,1}^2)h^2k_0^2 + [2 - 6iB_{\mu,0}hk_0 - (4B_{\mu,0}^2 - B_{\mu,1}^2)h^2k_0^2]r_0\right\}}{3B_{\mu,1}^2h^2k_0^2}, \tag{49}$$

and, as an extension, one can deduce that $r_n = s_n(r_0)$, with $n \geq -1$ and s_n a function depending on n. This property of the system means that there are no reflected waves of the form $e^{i|k_n|(x+c_0t)}$. However, for a non integer ratio of ω_p/ω this is no longer the case and it leads to harmonics with a reversed wave phase; it is visible from the rapid increase of the harmonic $|r_{-2}|$ from a practically zero value at $\omega_p/\omega = 1$ to the order of 10^{-4} when $\omega_p/\omega = 1.1$. It is also worth commenting on the fact that while in the Schrödinger equation the harmonics with $\omega_n < 0$ result in evanescent modes (see [13,15]), for the wave equation there is no restriction of that matter.

4.2. Quasistatic approximation

While Floquet theory gives a direct insight into the reproduced harmonics and their dependence on the frequency of oscillation, we have seen that we have small changes in the n-harmonic amplitude with ω_p for $n = -1, 0, 1$, implying the existence of a quasistatic (QS) regime ($\omega_p \to 0$) that needs to be examined.

In order to understand this quasistatic adiabatic limit, we focus on a barrier moving much slower than the period of the incident wave, such that $\omega_p \ll \omega$. Then, the static solution for the reflected and the transmitted waves given in Section 3.2 is modified only by adjusting the time-dependent blockage coefficient (Eq. (26)) in the relations (25). Hence, this yields

$$\tilde{f}_r(x,t) = -\frac{ikh(B_{\mu,0} + B_{\mu,1}\cos(\omega_p t))}{1 - ikh(B_{\mu,0} + B_{\mu,1}\cos(\omega_p t))}e^{-i(kx+\omega t)}, \tag{50}$$

$$\tilde{f}_t(x,t) = \frac{1}{1 - ikh(B_{\mu,0} + B_{\mu,1}\cos(\omega_p t))}e^{i(kx-\omega t)}, \tag{51}$$

with $\tilde{f}_r$ and $\tilde{f}_t$ denoting the reflected and transmitted wave in this adiabatic limit. Next, we Fourier expand the two components using the series

$$\tilde{f}_r = \sum_n \tilde{r}_n e^{i(kx-\omega_n t)}, \tag{52}$$

$$\tilde{f}_t = \sum_n \tilde{t}_n e^{i(kx-\omega_n t)}, \tag{53}$$

with $\omega_n = \omega + n\omega_p$. Combining Eqs. (50), (51) with Eqs. (52), (53), then projecting on $e^{-in\omega_p t}$ and using the orthogonality of the modes, one can express the coefficients $\tilde{r}_n$ and $\tilde{t}_n$ in the quasistatic approximation as

$$\tilde{r}_n = \frac{1}{T_p}\int_0^{T_p} \frac{ikh(B_{\mu,0} + B_{\mu,1}\cos(\omega_p t))}{ikh(B_{\mu,0} + B_{\mu,1}\cos(\omega_p t)) - 1}e^{-in\omega_p t}dt, \tag{54}$$

$$\tilde{t}_n = \frac{1}{T_p}\int_0^{T_p} \frac{1}{1 - ikh(B_{\mu,0} + B_{\mu,1}\cos(\omega_p t))}e^{in\omega_p t}dt. \tag{55}$$

By applying contour integration, which involves setting $\varphi = \omega_p t$ and then integrating over the unit circle with complex variable $z = e^{i\varphi}$, we obtain the expressions

$$\tilde{t}_n = \frac{\left(\beta/\gamma - \sqrt{(\beta/\gamma)^2 - 1}\right)^{-|n|}}{\sqrt{\beta^2 - \gamma^2}}, \tag{56}$$

$$\tilde{r}_n = \delta_{0n} - \frac{\left(\beta/\gamma - \sqrt{(\beta/\gamma)^2 - 1}\right)^{-|n|}}{\sqrt{\beta^2 - \gamma^2}}, \tag{57}$$

with $\beta = 1 - ikhB_{\mu,0}$ and $\gamma = ikhB_{\mu,1}$. Notice that the coefficients are symmetric around the fundamental, i.e. $\tilde{r}_n = \tilde{r}_{-n}$ for $n \neq 0$, which is not the case in the Floquet theory (see Fig. 6b,c). They are also independent from ω_p, as expected.

In order to test the robustness and the limitations of the QS approximation, as opposed to the Floquet theory, we once again fix the incidence frequency ω and vary ω_p. In Fig. 6a,b,c we illustrate the reflection amplitudes of each harmonic with index n when

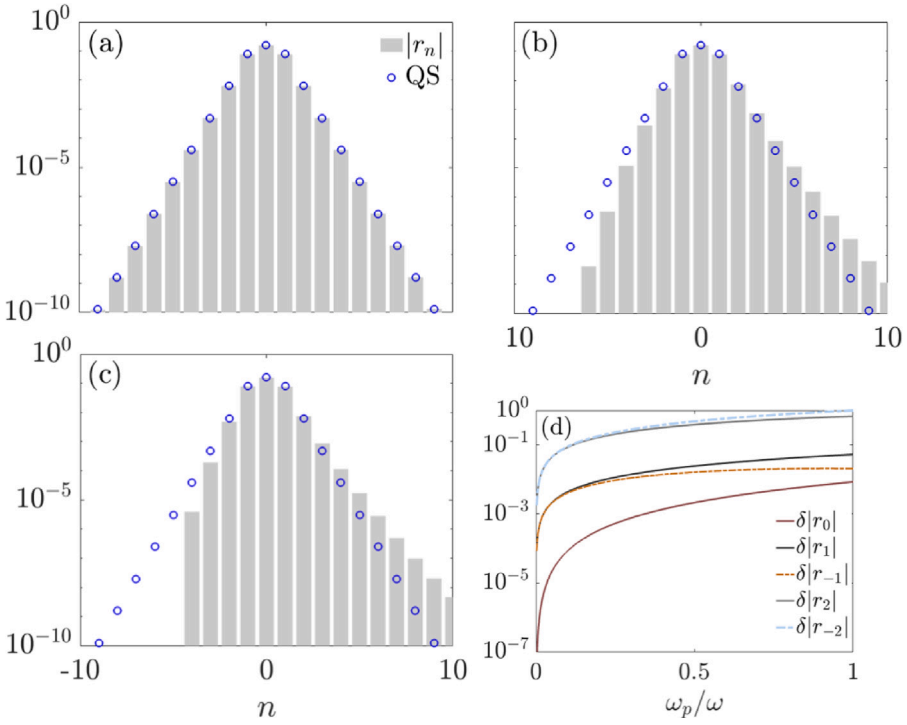

Fig. 6. Reflection amplitudes calculated by the Floquet theory (in gray bars) and by the QS approximation (in blue points) for $\omega\sqrt{h/g} = 0.1$, with (**a**) $\omega_p\sqrt{h/g} = \omega/1000$, (**b**) $\omega_p\sqrt{h/g} = \omega/6$ and (**c**) $\omega_p\sqrt{h/g} = \omega/4$. (**d**) Relative difference of the two methods in terms of ω_p/ω for the harmonics of indexes $-2 \le n \le 2$.

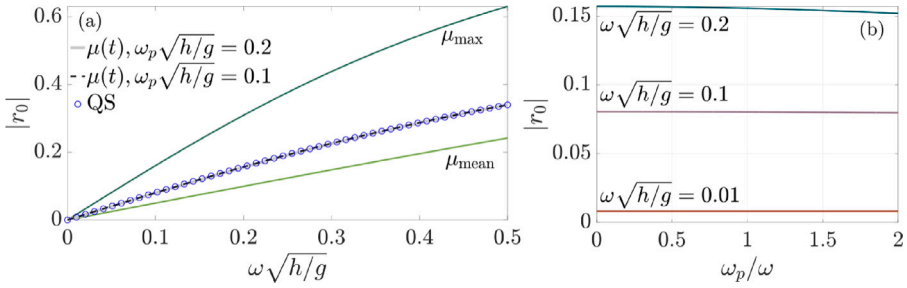

Fig. 7. (**a**) Comparison of the coefficient $|r_0|$ for a static plate of heights $\mu_{max} = 0.95, \mu_{mean} = 0.698$ with the oscillating plate of Fig. 4a where $\omega_p\sqrt{h/g} = 0.2, 0.1$, along with the quasistatic result (QS) given by Eq. (57). (**b**) Closer view of the change in $|r_0|$ with the normalized frequency of oscillation ω_p/ω for $\omega\sqrt{h/g} = 0.01, 0.1, 0.2$.

$\omega\sqrt{h/g} = 0.1$ for increasing values of ω_p. It is evident that the closer we move to the adiabatic limit where $\omega_p \ll \omega$ the better the agreement between the QS approximation and Floquet theory as a whole, while in all cases the harmonics at $n = -1, 0, 1$ are very well approximated by the QS approximation. A quantitative representation of the relative difference between the two methods, defined as $\delta|r_n| = ||r_n| - |\tilde{r}_n||/|\tilde{r}_n|$, is depicted in Fig. 6d for $n = -2, -1, 0, 1, 2$, spanning ω_p/ω from 0 to 1. For $\omega_p \to 0$, we see that $\delta|r_0| \sim 10^{-7}$, $\delta|r_{\pm1}| \sim 10^{-4}$ and $\delta|r_{\pm2}| \sim 10^{-3}$, whereas for the case of panel (c) where the mismatch is more visible, $\delta|r_0| \sim 5 \cdot 10^{-4}$ and increases to $\delta|r_{\pm2}| \sim 0.2$.

Focusing on the fundamental frequency $n = 0$, we wish now to inspect the effect of the plate when it is static versus when it is moving. Taking two limit values of μ, specifically the maximum height $\mu_{max} = 0.95$ and the mean value of $\mu(t)$, $\mu_{mean} = 0.698$, we detect that $|R_{sw,\mu_{mean}}| < |r_0| < |R_{sw,\mu_{max}}|$ for all values of ω (see Fig. 7a). Interestingly, the coefficient $|r_0|$ is also minimally affected with changes of ω_p, as already discussed in Section 4.1.1, and is almost perfectly captured by the result given from the quasistatic approximation. Arguably, a slight deviation from this quasistatic result can be achieved for higher values of ω and working towards fastest plate oscillations, i.e by challenging the limits of the shallow water approximation. This remark can be made by viewing Fig. 7b, where we find a relative variation of just 10^{-8} for $\omega\sqrt{h/g} = 0.01$, of 10^{-2} for $\omega\sqrt{h/g} = 0.1$ and of $3 \cdot 10^{-2}$ for $\omega\sqrt{h/g} = 0.2$ in an interval of $\omega_p/\omega \in [0, 2]$.

5. Conclusion

In this paper we proposed a Floquet theory approach for the reflection and transmission of a plane wave from a vertically oscillating plate in the low frequency approximation. With this shallow water approximation this oscillation of the plate is reduced to a 1D model with the simple wave equation and a time-varying point discontinuity condition at the plate location. We show that even a slowly oscillating plate can have an important impact on the generation of reflected harmonics, notably the first sidebands ($n = \pm 1$) whose amplitude reaches close to 50% the one of the fundamental one ($n = 0$). When considering the quasistatic adiabatic limit $\omega_p \ll \omega$, explicit relations can be derived for the amplitudes of all harmonics which strongly agree with the full Floquet theory up to $n = \pm 2$ for $\omega_p \to 0$. In addition, the reflection coefficient of the fundamental is nicely matched with the quasistatic result for all incident frequencies, and a slight variation when modifying ω_p can be only achieved by moving to higher frequencies and imposing even faster oscillations. This quasistatic value lies between the maximum and the mean value of the height oscillation. Overall, we conclude that the quasistatic approximation is surprisingly robust and can efficiently predict the behavior of the system with respect to the reflection coefficient of the fundamental harmonic regardless of the characteristic frequency of oscillation as long as the shallow water approximation is valid.

CRediT authorship contribution statement

Magdalini Koukouraki: Formal analysis, Writing – original draft. **Philippe Petitjeans:** Supervision, Writing – review & editing. **Agnès Maurel:** Methodology, Supervision, Writing – review & editing. **Vincent Pagneux:** Methodology, Supervision, Writing – review & editing.

Declaration of competing interest

The authors declare that they have no known competing financial interests or personal relationships that could have appeared to influence the work reported in this paper.

Acknowledgements

The authors acknowledge the support of the ANR under grant no. ANR-21-CE30-0046 CoProMM.

Data availability

Data will be made available on request.

References

[1] G. Ptitcyn, M.S. Mirmoosa, A. Sotoodehfar, S.A. Tretyakov, A tutorial on the basics of time-varying electromagnetic systems and circuits: Historic overview and basic concepts of time-modulation, IEEE Antennas Propag. Mag. 65 (2023) 10–20.
[2] K.A. Lurie, An Introduction to the Mathematical Theory of Dynamic Materials, vol. 15, Springer, New York, 2007.
[3] Z. Hayran, F. Monticone, Using time-varying systems to challenge fundamental limitations in electromagnetics: Overview and summary of applications, IEEE Antennas Propag. Mag. 65 (2023) 29–38.
[4] V. Pacheco-Peña, D.M. Solís, N. Engheta, Time-varying electromagnetic media: opinion, Opt. Mater. Express 12 (2022) 3829–3836.
[5] V. Bacot, M. Larousse, A. Eddi, M. Fink, E. Fort, Time reversal and holography with spacetime transformations, Nat. Phys. 12 (2016) 972.
[6] B. Apffel, E. Fort, Frequency conversion cascade by crossing multiple space and time interfaces, Phys. Rev. Lett. 128 (2022) 064501.
[7] E. Galiffi, R. Tirole, S. Yin, H. Li, S. Vezzoli, P.A. Huidobro, M.G. Silveirinha, R. Sapienza, A. Alu, J.B. Pendry, Photonics of time-varying media, Adv. Photonics 4 (2022) 014002.
[8] I. Kiorpelidis, F.K. Diakonos, G. Theocharis, V. Pagneux, Transient amplification in stable floquet media, Phys. Rev. B 110 (2024) 134315.
[9] V. Pacheco-Peña, N. Engheta, Temporal aiming, Light. Sci. Appl. 9 (2020) 129.
[10] F.R. Morgenthaler, Velocity modulation of electromagnetic waves, IRE Trans. Microw. Theor. Tech. 6 (1958) 167–172.
[11] N. Engheta, Four-dimensional optics using time-varying metamaterials, Science 379 (2023) 1190.
[12] V. Yakubovich, V. Starzhinskii, Linear Differential Equations with Periodic Coefficients, John Wiley Sons, New York, 1975.
[13] L. Wenjun, L.E. Reichl, Floquet scattering through a time-periodic potential, Phys. Rev. B 60 (1999) 15732–15741.
[14] D.F. Martinez, L.E. Reichl, Transmission properties of the oscillating δ-function potential, Phys. Rev. B 64 (2001) 245315.
[15] P.A. Pantazopoulos, N. Stefanou, Layered optomagnonic structures: Time floquet scattering-matrix approach, Phys. Rev. B 99 (2019) 144415.
[16] G.F. Fitz-Gerald, The reflection of plane gravity waves travelling in water of variable depth, Proc. R. Soc. Lond. A Math. Phys. Sci. 284 (1976) 49–89.
[17] J. Hamilton, Differential equations for long-period gravity waves on fluid of rapidly varying depth, J. Fluid Mech. 83 (1977) 289–310.
[18] D.V. Evans, C.M. Linton, On step approximations for water-wave problems, J. Fluid Mech. 278 (1994) 229–249.
[19] R. Porter, D. Porter, Approximations to the scattering of water waves by steep topography, J. Fluid Mech. 562 (2006) 279–302.
[20] J.N. Newman, Interaction of water waves with two closely spaced vertical obstacles, J. Fluid Mech. 66 (1974) 97–106.
[21] R. Porter, D.V. Evans, Complementary approximations to wave scattering by vertical barriers, J. Fluid Mech. 294 (1995) 155–180.
[22] C. Marangos, R. Porter, Shallow water theory for structured bathymetry, Proc. R. Soc. A 477 (2021) 20210421.
[23] A. Maurel, K. Pham, J.J. Marigo, Scattering of gravity waves by a periodically structured ridge of finite extent, J. Fluid Mech. 871 (2019) 350–376.
[24] A. Maurel, J.J. Marigo, P. Cobelli, P. Petitjeans, V. Pagneux, Revisiting the anisotropy of metamaterials for water waves, Phys. Rev. B 96 (2017) 134310.
[25] D.V. Evans, Diffraction of water waves by a submerged vertical plate, J. Fluid Mech. 40 (1970) 433–451.
[26] E.O. Tuck, Some Classical Water-Wave Problems in Varying Depth, Waves on Water of Variable Depth, Springer, Berlin, Heidelberg, 2005, pp. 9–20.
[27] C.C. Mei, M. Stiassnie, D.K.P. Yue, Theory and Applications of Ocean Surface Waves. Part 1: Linear Aspects, vol. 23, World Scientific, Singapore, 2005.
[28] G.B. Whitham, Linear and Nonlinear Waves, John Wiley Sons, New York, 1974.
[29] H. Lamb, Hydrodynamics, Sixth ed., Cambridge University Press, Cambridge, 1932.
[30] J.J. Stoker, Water Waves, the Mathematical Theory with Applications, Interscience Publishers, New York, 1957.
[31] J. Gazalet, S. Dupont, J.C. Kastelik, Q. Rolland, B. Djafari-Rouhani, A tutorial survey on waves propagating in periodic media: Electronic, photonic and phononic crystals. perception of the bloch theorem in both real and fourier domains, Wave Motion 50 (3) (2013) 619–654.